Available online at www.sciencedirect.com
SCIENCE DIRECT®
Journal of Solid State Chemistry 176 (2003) 37–46
JOURNAL OF SOLID STATE CHEMISTRY
http://elsevier.com/locate/jssc

Preparation, phase transition and thermal expansion studies on low-cristobalite type $Al_{1-x}Ga_xPO_4$ ($x = 0.0$, 0.20, 0.50, 0.80 and 1.00)

S.N. Achary,[a] O.D. Jayakumar,[b] A.K. Tyagi,[a,*] and S.K. Kulshresththa[b]

[a] *Applied Chemistry Division, Bhabha Atomic Research Centre, Mumbai 400 085, India*
[b] *Novel Materials and Structural Chemistry Division, Bhabha Atomic Research Centre, Mumbai 400 085, India*

Received 15 April 2003; received in revised form 3 June 2003; accepted 6 June 2003

Abstract

The orthorhombic (α) low-cristobalite type $AlPO_4$ and $GaPO_4$ and their solid solutions are prepared by co-precipitation followed by high temperature annealing of the precipitate. The single phasic nature of the products is ascertained by powder XRD at room temperature. The high temperature behavior of these samples is studied by HT-XRD over the temperature range of 25–1000°C. All these compositions undergo an orthorhombic to cubic (β, high-cristobalite) phase transition at elevated temperature. The unit cell parameters at different temperatures are determined by refining the observed powder diffraction profiles. The phase transition is accompanied by a significant increase in the unit cell volume, leading to the formation of a low dense structure. The variation of unit cell volume with temperature for each composition shows that the orthorhombic phase has a significantly larger thermal expansion than the cubic (high temperature) phase. The high temperature behavior of all the compositions except the $GaPO_4$ is similar. $GaPO_4$ undergoes a phase separation to a more stable quartz type phase above 800°C. However, the quartz type phase again transforms to the high cristobalite (β) phase at 1000°C. Thermal expansions of all these phases are explained in term of the variation of M–O–P angle as a function of temperature.

Keywords: Phase transition; Thermal expansion; Phosphates; Cristobalite; High temperature XRD

1. Introduction

Thermal expansion is an important property, generally considered for any material to be used at elevated temperatures. An increase in an-harmonic potential with increasing temperature causes the thermal expansion of chemical bonds, which in turn results in dilation of crystal lattice. However, there are several unusual examples where despite the expansion of the chemical bonds, there is either an overall contraction in the lattice (negative thermal expansion, NTE) or a very small or no expansion at all (low or zero thermal expansion, LTE or ZTE). Such anomalous thermal expansion behavior has been reported for several phosphates, tungstates and molybdates [1–5]. The negative thermal expansion behavior of tungstate, molybdate and phosphates crystals has been explained on the basis of transverse vibrations of the bridging oxygen, in M–O–M' [6]. The compounds with framework architecture of the building polyhedra mostly form low density structures, where the rocking of the polyhedra leads to the possibility of anomalous, namely anisotropic, low or negative thermal expansion [6]. The negative or low thermal expansion behavior is also reported in silica [7], ice [8] and zeolites [9]. Recently, a very large negative thermal expansion was reported in $AlPO_4$ with zeolite like frame [10]. In general it is desirable to have materials with zero thermal expansion so as to have practical applications. The negative thermal expansion materials are generally used as stress absorbing materials, as they can act as buffer to compensate the unwanted expansion in the both mechanical and electronics components at higher temperatures.

Both $AlPO_4$ and $GaPO_4$ are the derivatives of quartz structure and are obtained by replacing half of the Si by Al and the other half by P atoms. The structure of these compounds contain both $[(Al/Ga)O_4]^{3+}$ and $(PO_4)^{3-}$ tetrahedral units and the four oxygens of PO_4^{3-} are connected to four metal ions. Both $AlPO_4$

*Corresponding author. Fax: +91-22-2550-5151/2551-9613.
E-mail address: aktyagi@magnum.barc.ernet.in (A.K. Tyagi).

0022-4596/$ - see front matter © 2003 Elsevier Inc. All rights reserved.
doi:10.1016/S0022-4596(03)00341-4

and $GaPO_4$ crystallize in all types of lattices of SiO_2 [11–15]. The cristobalite (orthorhombic) lattice for $AlPO_4$ and $GaPO_4$ is observed at elevated temperature. However, the orthorhombic structure can be retained at room temperature after cooling, if the sample is annealed for a longer time above the cristobalite transition temperature. The structures of the low cristobalite phase of both $AlPO_4$ and $GaPO_4$ have almost similar unit cell dimensions. Both Al/Ga and P occupy crystallographically unique sites and oxygen ions are placed at two distinct sites [16]. The fairly close lattice parameters of the two end members, $AlPO_4$ and $GaPO_4$, and the small difference of ionic radii of Al^{3+} and Ga^{3+} [17] suggest the possibility of solid solution formation over the complete range of compositions.

Although, several reports pertaining to the thermal expansion behavior of quartz type $AlPO_4$ [18] and $GaPO_4$ [19] exist in literature, the crystal structure of high cristobalite type $AlPO_4$ and $GaPO_4$ were not known conclusively for a long time. Later Ng and Calvo had conclusively reported [20] the crystal structure of high (β) cristobalite. In that investigation they had also reported the high temperature unit cell parameters of both low (α) and high (β) cristobalite type $AlPO_4$ [20]. The kinetics of phase transition from α to β cristobalite type $GaPO_4$ was also reported [21], but without the details of the unit cell expansion behavior. Besides, no data dealing with high temperature behavior of the mixed composition phosphates are available. The mixed composition lattice is expected to reflect the influence of a gradual variation of average ionic radii on thermal expansion behavior. The present report deals with the study of the phase transition and variation of the unit cell parameters as a function of temperature for $Al_{1-x}Ga_xPO_4$ samples with $0.0 \leqslant x \leqslant 1.0$ with a view to see the effect of the change in the ionic radius of metal ions on the stability of low and high cristobalite phases as well as on the magnitude of the thermal expansion coefficients of these phases.

2. Experimental

The amorphous precipitates of $AlPO_4$, $GaPO_4$ and $Al_{1-x}Ga_xPO_4$ compositions are obtained by adding NH_4OH to the aqueous solutions of metal chlorides and H_3PO_4. The precipitates are dried at about 175°C and then annealed at 1300°C for about 24 h in a re-crystallized alumina crucible. The colorless products obtained are characterized by powder XRD patterns recorded on a Philips powder X-ray diffractometer (model PW1710) using the Cu$K\alpha$ radiation. The XRD patterns of the samples at other temperatures are recorded on a Philips X-Pert Pro diffractometer, with Anton Parr high temperature attachment. Each well ground sample is mounted on a platinum strip, which serves the purpose of both sample holder as well as heater. The temperature is controlled with Eurotherm temperature programmer, with an accuracy of ± 1°C. Each sample is heated to the desired temperature at the rate of 20°C/min and held for 5 min. The XRD patterns are recorded within the 2θ range of 10–80° with step width of 0.02° and step time of 0.5 s using Cu$K\alpha$ radiation. The diffracted beam is monochromatized with curved graphite monochromator.

The observed profile of the XRD pattern is refined using Rietveld refinement program Fullprof [22]. The profile is fitted with Pseudo-Voigt profile function. The profile refinement was started with scale and background parameters followed by the unit cell parameters. The typical half width parameters, mixing parameter and preferred orientation parameter are also refined. Subsequently, the peak asymmetry was also corrected. After getting a proper match in the profile model, the positional parameters and overall thermal parameters were refined. The profile of the powder XRD pattern recorded at various temperatures and various compositions are similarly refined. The goodness of the refinements was observed by the residuals (R-values).

3. Results and discussion

A comparison of the observed room temperature powder XRD pattern for $AlPO_4$ and $GaPO_4$ with the reported JC-PDS cards 11–500 and 31–546, respectively, revealed their phase purity. Both of these materials crystallize in the low cristobalite (orthorhombic) lattice. The comparison of the XRD patterns of these compounds with those of the other mixed metal ion compositions indicates the perfect solid solution formation between these two end members. The solid solution in the complete range between $GaPO_4$ and $AlPO_4$ can be expected owing to the similarity in their lattice type and marginal difference in ionic radii of the corresponding metal ions ($Al^{3+} = 0.53$ and Ga^{3+} 0.62 Å in tetrahedral coordination). The preliminary results of the solid solution formation were earlier reported on the basis of the powder XRD and ^{31}P NMR studies [23].

The phases observed for different compositions are characterized on the basis of the Rietveld refinement. The initial position parameters and the space group ($C222_1$) for the orthorhombic phase are taken from the values reported by Mooney [16] for $AlPO_4$ and $GaPO_4$ (low-cristobalite). It can be mentioned here that the isotropic thermal parameters of individual atoms are not refined. The typical unit cell parameters and other detailed refined crystallographic parameters for $AlPO_4$ and $GaPO_4$ are given in Table 1. The observed unit cell parameters are also found to have a good agreement with the earlier reported values [Ref. [16], JC-PDS

Table 1
Typical refined crystallographic parameters for the room temperature phase of $Al_{1-x}Ga_xPO_4$

	$AlPO_4$	$Al_{0.8}Ga_{0.2}PO_4$	$Al_{0.5}Ga_{0.5}PO_4$	$Al_{0.2}Ga_{0.8}PO_4$	$GaPO_4$
Temperature	RT (25°C)	RT (25°C)	RT (25°C)	RT (25°C)	RT (25°C)
Cryst. sys.[a]	Ortho.	Ortho.	Ortho.	Ortho.	Ortho.
a (Å)	7.0843(14)	7.0529(12)	7.0295(12)	6.9968(5)	6.9876(5)
b (Å)	7.0823(13)	7.0558(11)	7.0173(11)	6.9794(5)	6.9624(5)
c (Å)	6.9989(4)	6.9551(3)	6.9217(5)	6.8884(3)	6.8774(4)
V (Å^3)	351.15(9)	346.11(8)	341.44(8)	336.38(4)	334.59(4)
M[b]: $4b(0, y, 1/4)$					
y	0.194(1)	0.198(1)	0.191(1)	0.185(1)	0.186(1)
P: $4a(x, 0, 0)$					
x	0.295(1)	0.205(1)	0.299(2)	0.309(1)	0.316(2)
O1: $8c(x, y, z)$					
x	0.187(1)	0.191(1)	0.189(2)	0.200(1)	0.202(2)
y	0.058(2)	0.048(1)	0.040(2)	0.033(1)	0.026(2)
z	0.163(1)	0.167(1)	0.170(2)	0.171(1)	0.187(2)
O2: $8c(x, y, z)$					
x	0.428(2)	0.428(1)	0.429(2)	0.440(1)	0.441(2)
y	0.160(1)	0.159(1)	0.156(2)	0.160(1)	0.171(2)
z	0.946(1)	0.952(1)	0.964(2)	0.964(1)	0.969(2)
$B_{overall}$	1.67(7)	1.32(6)	0.68(7)	1.29(6)	[c]
R_p	13.6	12.6	13.7	12.5	13.4
R_{wp}	19.0	17.7	20.2	19.4	18.0
R_{exp}	15.5	15.8	15.5	14.3	15.0
χ^2	1.5	1.3	1.7	1.8	1.4
R_B	3.8	4.1	6.6	4.2	7.4

[a] Space group: $C222_1$ (No. 20) and $Z = 4$.
[b] $M = Al^{3+}/Ga^{3+}$.
[c] B_{iso} values: Ga: 1.7(1), P: 1.1(4), O1: 1.61 and O2: 1.61.

No. 11–500 and 31–546]. The observed and calculated XRD patterns along with the difference plot for $AlPO_4$ and $GaPO_4$ are shown in Figs. 1(a) and 2(a), respectively. The typical values of the refined structural parameters and unit cell parameters for the room temperature phases of all the other compositions are also included in Table 1. Although, the ionic radius of the Ga^{3+} is larger than that of Al^{3+}, $GaPO_4$ crystallizes with lattice of a smaller unit cell volume than $AlPO_4$. This can be noted from the observed unit cell volume of the two phases (unit cell volume of $AlPO_4$ and $GaPO_4$ are 351.2(1) and 334.6(0) Å^3 respectively, $Z = 4$). Besides, the average bond length of Ga–O (1.85 Å) is also higher than the Al–O bond length (1.77 Å). The larger unit cell volume of the $AlPO_4$ can be attributed to the Al–O–P angles (average = 145°), which is higher than the Ga–O–P angle in $GaPO_4$ (average = 132°). The higher value of Al–O–P angle causes the larger separation of the Al and P distances as compared to Ga and P, leading to a larger unit cell volume for the former. The gradual replacement of the Al^{3+} by the Ga^{3+} ion indicates a gradual decrease of the unit cell volume with compositions. A comparison of the observed unit cell parameters of various nominal compositions for the room temperature phases is shown in Table 1, where the detailed crystallographic parameters of all the studied compositions are listed.

The typical unit cell parameters of $AlPO_4$ at higher temperature (viz. 100°C, 200°C) are obtained by refining the observed XRD patterns with starting values taken from the calculated parameters for the room temperature phase. The XRD pattern of $AlPO_4$ recorded at 300°C is found to be drastically different from those recorded at the lower temperatures, indicating the phase transition. Since in order to follow the thermal expansion behavior, the HT-XRD patterns are recorded at 100°C interval, the exact temperature of phase transition could not be delineated. Again in order to avoid the presence of mixed phase XRD patterns, the intermediate temperatures are avoided. The observed reflections for this phase indicate the formation $AlPO_4$ (high cristobalite phase).

The structural details of the high cristobalite phase of the $AlPO_4$ were earlier reported by Wright and Leadbetter [24] and Ng and Calvo [20]. It can be mentioned here that the lattices of high (β) cristobalite type $AlPO_4$ and $GaPO_4$ are similar to that of the SiO_2 (cristobalite) phase. However, the structure of SiO_2 is explained with the space group Fd3 m, whereas, the former two structures are explained with the space group $F-43m$ [20,15]. The observed XRD pattern for $AlPO_4$ at 300°C is refined by Rietveld method with the positional parameters taken form the study of Ng and Calvo [20] (Al^{3+}: 4a, P^{5+}: 4c and O: 48h, $occ.$ 1/3). In

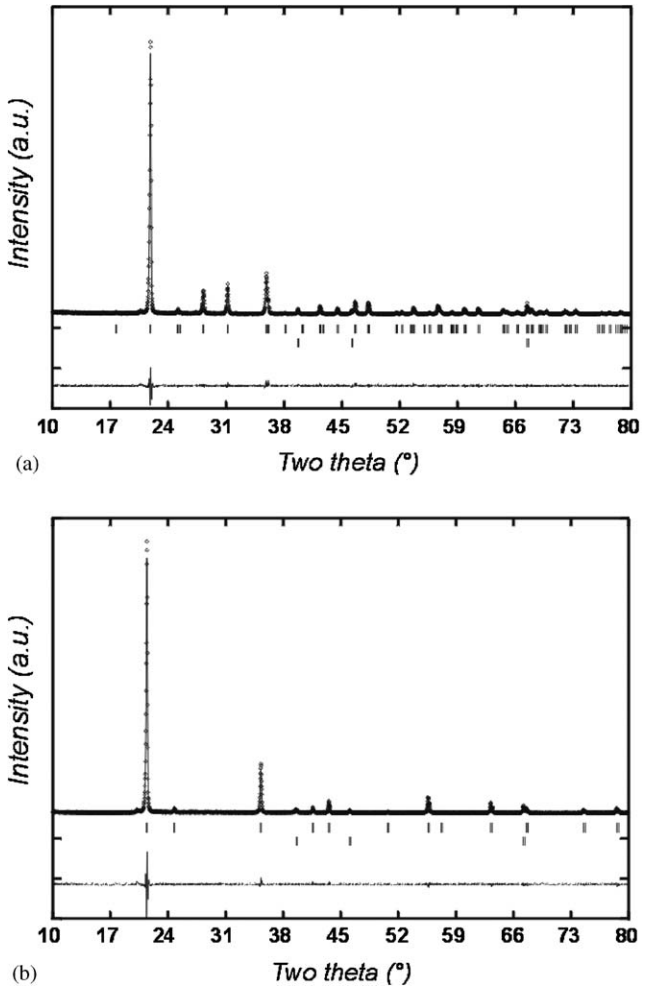

Fig. 1. The observed and calculated XRD patterns of $AlPO_4$ at 25°C (a) and 300°C (b).

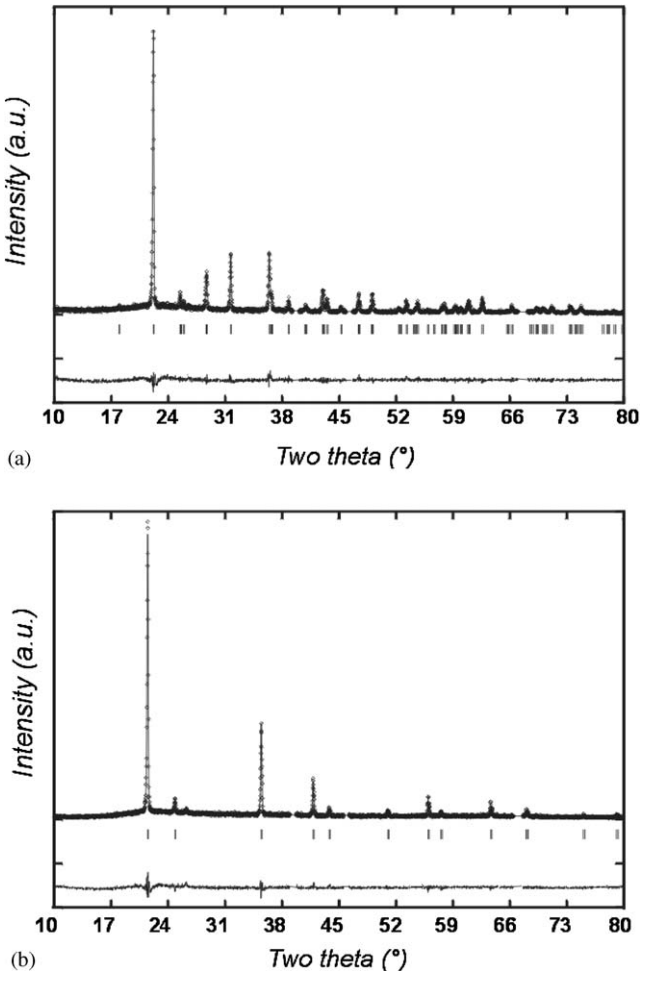

Fig. 2. The observed and calculated XRD patterns of $GaPO_4$ at 25°C (a) and 700°C (b).

this refinement too, only the overall thermal parameters are refined. The refined structural parameters of $AlPO_4$ at 300°C are shown in Table 2, and the values are in good agreement with those reported by Wright and Leadbetter [24] and Ng and Calvo [24]. The typical observed and calculated XRD patterns along with the difference plot are shown in Fig. 1(b). In a similar manner the XRD pattern recorded at 700°C for $GaPO_4$ shows the high cristobalite modification. The typical observed and calculated XRD patterns for high cristobalite type $GaPO_4$ are shown in Fig. 2(b). In an identical manner the high cristobalite lattice of all other nominal compositions are obtained and the unit cell parameter and other structural parameters are given in Table 2. The unit cell parameters at different temperatures are also obtained in a similar manner.

A systematic variation of the unit cell parameters with temperature for both the low temperature and high temperature phase of $AlPO_4$ and $GaPO_4$ are shown in Figs. 3 and 4, respectively. The variation of the unit cell parameters for the orthorhombic phase (α-phase) shows a gradual increase with the increase in temperature. The phase transition is accompanied with an abrupt expansion in the unit cell volume. It may be mentioned here that the unit cell of both α and β phases represent four formula units of $AlPO_4$ or $GaPO_4$ (i.e., $Z = 4$). The variation of the unit cell parameter in the cubic (β) phase suggests a significantly lower thermal expansion. This striking feature is also reflected in the variation of the unit cell volume with temperature, for both the phases. The typical coefficient of volume thermal expansion of the $AlPO_4$ in the temperature range of 25–200°C is 100×10^{-6}/°C and that of the cubic phase (within the temperature range of 300–1000°C) has a drastically lower value, i.e., 5.8×10^{-6}/°C. The large difference in the unit cell volume of the orthorhombic and the cubic phase implies a significant decrease in the density of the unit cell. The other nominal compositions namely, $Al_{0.8}Ga_{0.2}PO_4$, $Al_{0.5}Ga_{0.5}PO_4$ and $Al_{0.2}Ga_{0.8}PO_4$ also have similar thermal expansion behavior. In all these cases a drastic expansion of the unit cell volume occurred at the phase transition. All the studied nominal

Table 2
Typical refined crystallographic parameters for the high temperature phase of $Al_{1-x}Ga_xPO_4$

	$AlPO_4$	$Al_{0.8}Ga_{0.2}PO_4$	$Al_{0.5}Ga_{0.5}PO_4$	$Al_{0.2}Ga_{0.8}PO_4$	$GaPO_4$
Temperature	300°C	300°C	400°C	600°C	700°C
Cryst. sys.[a]	Cubic	Cubic	Cubic	Cubic	Cubic
A (Å)	7.1969(2)	7.1665(2)	7.1561(2)	7.1503(2)	7.1850(2)
V (Å^3)	372.77(1)	368.06(2)	366.47(2)	365.57(2)	366.76(2)
M[b]: 4a(0, 0, 0)					
P: 4c(1/4, 1/4, 1/4)					
O1: ([c])					
48h(x, x, z)					
x	0.114(1)	0.112(1)	0.112(1)	0.111(1)	0.106(2)
z	0.188(1)	0.196(1)	0.202(1)	0.205(1)	0.207(5)
$B_{overall}$	4.31(12)	4.44(10)	4.92(12)	5.71(11)	[d]
R_p	13.4	13.8	11.3	13.6	11.6
R_{wp}	18.3	18.9	20.2	18.2	15.9
R_{exp}	12.1	14.1	15.0	12.1	11.5
χ^2	2.3	1.8	1.8	2.3	1.9
R_B	1.7	2.9	3.5	3.2	5.6

[a] Space group: F-43m (No. 216) and $Z = 4$.
[b] $M = Al^{3+}/Ga^{3+}$.
[c] Occupancy = 1/3.
[d] B_{iso} values Ga: 6.4(3), P: 5.4(6) and O: 6.7(1.0).

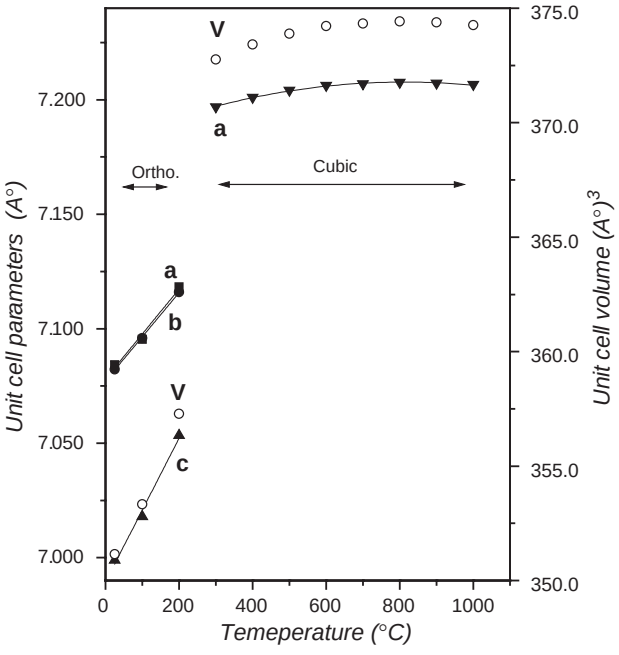

Fig. 3. Variation of unit cell parameters of $AlPO_4$ with temperature (accuracy: ±0.001 for orthorhombic phase and ±0.0002 for cubic phase).

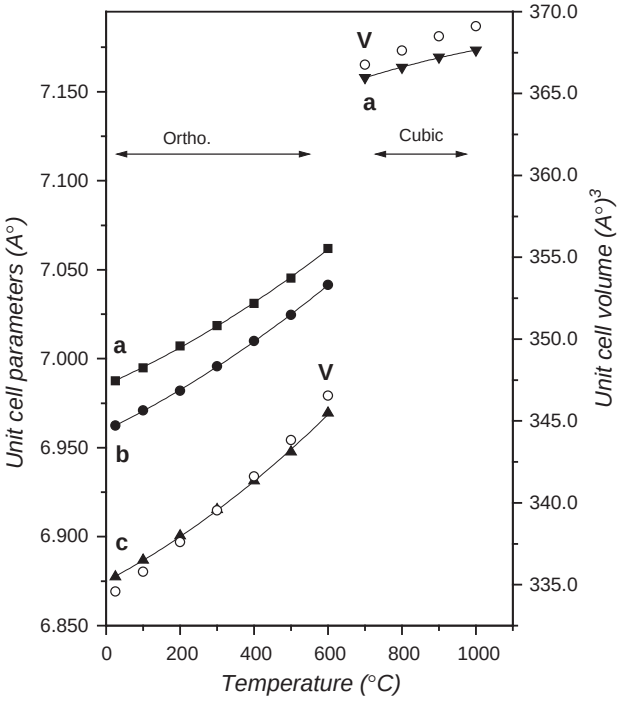

Fig. 4. Variation of unit cell parameters of $GaPO_4$ with temperature (accuracy: ±0.001 for orthorhombic phase and ±0.0002 for cubic phase).

compositions, except $GaPO_4$, have a similar orthorhombic to cubic phase transition. The typical powder XRD patterns of α and β phase of nominal composition $Al_{0.5}Ga_{0.5}PO_4$ are shown in Figs. 5(a) and (b). The variation of the unit cell parameters with temperature for this composition is shown in Fig. 6. The values of the thermal expansion coefficients of various other compositions over different temperature ranges have been summarized in Table 3.

The high temperature behavior of the orthorhombic phase of $GaPO_4$ is different from the rest of the compositions in this series. The α-cristobalite phase of

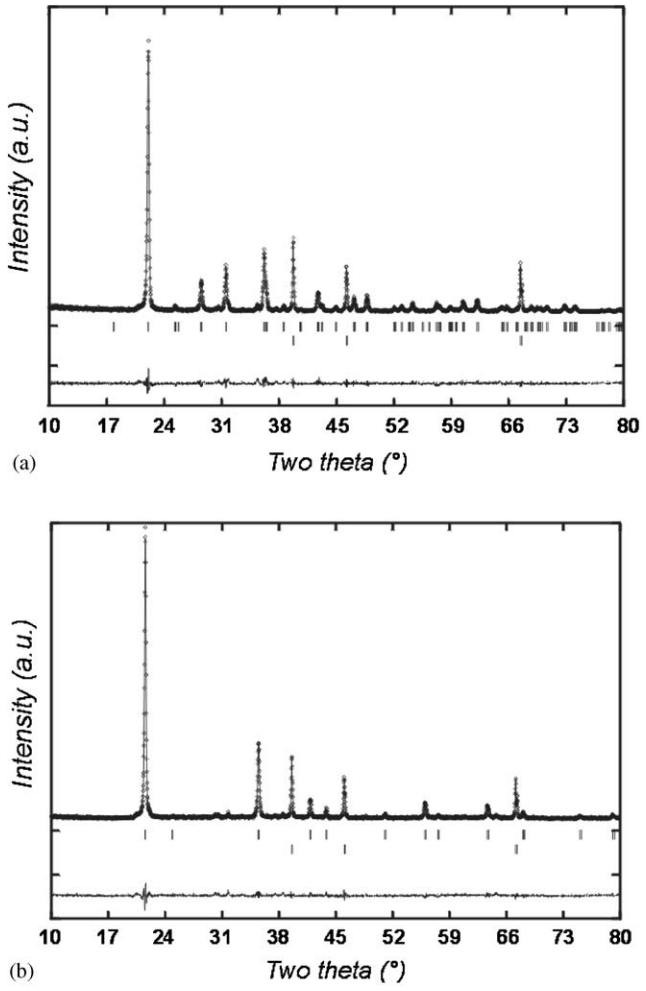

Fig. 5. The observed and calculated XRD patterns of $Al_{0.5}Ga_{0.5}PO_4$ at 25°C (a) and 400°C (b).

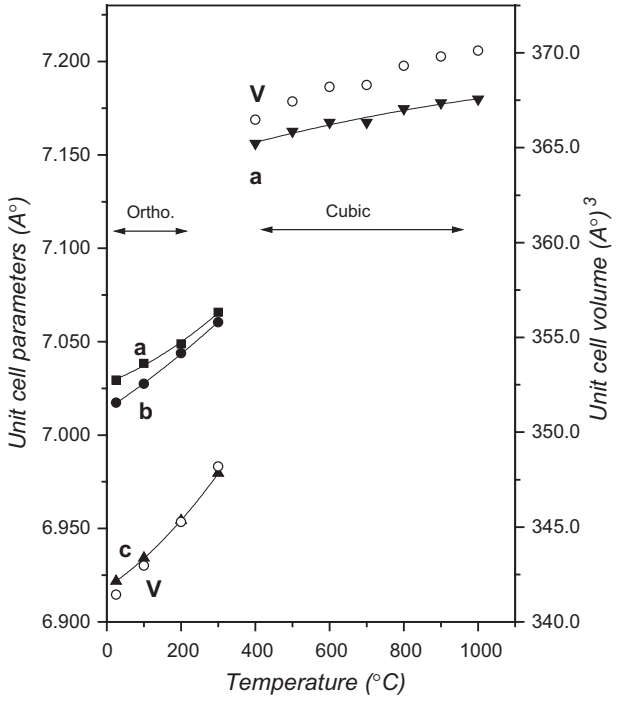

Fig. 6. Variation of unit cell parameters of $Al_{0.5}Ga_{0.5}PO_4$ with temperature (accuracy: ± 0.001 for orthorhombic phase and ± 0.0002 for cubic phase).

the $GaPO_4$ although transforms to the β-cristobalite lattice at 700°C, but at still higher temperature a phase transformation to the quartz type phase along with the β-cristobalite phase is observed. However, at 1000°C only the β-cristobalite type phase is observed. Thus, the XRD patterns recorded at the 800°C and 900°C show the presence of the two phases. The XRD patterns of the sample cooled to room temperature (25°C) from 800°C to 900°C show the complete reversal of the cristobalite to quartz type (low) phase. The observed XRD pattern of $GaPO_4$ sample cooled from 800°C is fitted with reported structural model for low-quartz type $GaPO_4$ [25]. The observed and calculated profiles along with the difference plot are shown in Fig. 7 and the typical refined parameters for this phase are given in Table 4. A typical XRD pattern of the $GaPO_4$ at 900°C is shown in Fig. 8, which shows the presence of both the quartz and high cristobalite phases. These facts imply that the quartz type $GaPO_4$ has higher stability than the low and high cristobalite form of $GaPO_4$. Hence, the quartz type $GaPO_4$ is easily obtained from the cristobalite form. Also, it is observed that the quartz type $GaPO_4$ has higher stability than the quartz type phase of either $AlPO_4$ or $Al_{1-x}Ga_xPO_4$ compositions. It is reported that the quartz type $GaPO_4$ transforms to β-cristobalite phase above 933°C [26]. Hence the XRD pattern of the $GaPO_4$ recorded at 1000°C show the presence of only the β-cristobalite phase. Except $GaPO_4$, all the other compositions reverted to their original α-cristobalite phase on cooling to room temperature after heating at 1000°C. The XRD pattern of $GaPO_4$ recorded at room temperature after heating at 1000°C showed the presence of both α- and β-cristobalite phase. To recover pure α-cristobalite type $GaPO_4$ the retrieved sample has to be annealed for long time at elevated temperature, which is the procedure, followed for the preparation of orthorhombic $GaPO_4$ in this study.

A comparison of the XRD patterns recorded at various temperatures for different studied compositions reveals that the phase transition temperature for low-cristobalite to high cristobalite type phase increases with the Ga^{3+} content in the lattice. It can be mentioned here that the typical transition temperature for $AlPO_4$ and $GaPO_4$ are reported as 210°C [13] and 590–633°C [26–28], respectively. The low and high cristobalite structures are almost similar except the relative orientation of the MO_4 and PO_4 tetrahedra. The correlated rotation of the MO_4 and PO_4 tetrahedra brings about the symmetry change. Hatch et al. [29] have reported the detailed symmetry analysis of this phase transition for

Table 3
Thermal expansion coefficient for $Al_{1-x}Ga_xPO_4$ over different temperature regions

	Temp. range (°C)	Crystal sym.	$\alpha_a \times 10^6$/°C	$\alpha_b \times 10^6$/°C	$\alpha_c \times 10^6$/°C	$\alpha_V \times 10^6$/°C
$AlPO_4$	25–200	O	27.4	27.2	44.5	99.8
	300–1000	C	1.93	—	—	5.75
	25–1000[a]	—	—	—	—	67.5
$Al_{0.8}Ga_{0.2}PO_4$	25–200	O	23.0	20.3	35.4	79.1
	300–1000	C	4.11	—	—	12.3
	25–1000[a]	—	—	—	—	74.5
$Al_{0.5}Ga_{0.5}PO_4$	25–300	O	18.7	22.4	30.4	71.9
	400–1000	C	5.52	—	—	16.6
	25–1000[a]	—	—	—	—	86.1
$Al_{0.2}Ga_{0.8}PO_4$	25–500	O	18.8	20.3	25.9	65.6
	600–1000	C	6.40	—	—	19.3
	25–1000[a]	—	—	—	—	97.6
$GaPO_4$	25–600	O	18.5	19.8	23.2	62.2
	700–1000	C	7.17	—	—	21.4
	25–1000[a]	—	—	—	—	105.8

[a] Represent the average thermal expansion coefficients derived from the unit cell volume of the orthorhombic and cubic phase obtained at 25°C and 1000°C.

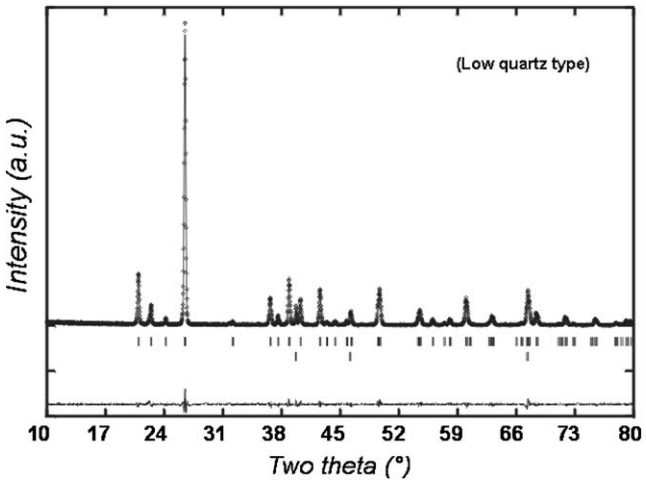

Fig. 7. The observed and calculated XRD patterns of low quartz type $GaPO_4$ (pattern recorded at room temperature after cooling from 800°C).

Table 4
Typical refined parameters for low-quartz type $GaPO_4$

Sample description	$GaPO_4$ Heated to 800°C and cooled to room temeparture
Temperature	25°C
Crystal system	Rhombohedral
Space group	$P3_121$ (No. 152)
a and c (Å)	4.9028(1) and 11.0456(4)
V (Å^3) and Z	229.94(1), 3
Ga: $3a(x,0,1/3), x$	0.4566(7)
B_{iso}	0.92(7)
P: $3b(x,0,5/6) : x$	0.458(2)
B_{iso}	0.17(11)
O1: $6c(x,y,z)$	0.398(2), 0.324(2), 0.3960(7)
B_{iso}	1.33(33)
O2: $6c(x,y,z)$	0.398(2), 0.267(1), 0.8716(9)
B_{iso}	1.23(31)
R_p	11.0%
R_{wp}	17.3%
R_{exp}	13.66%
χ^2	1.61
R_B	2.99
Typical bond lengths (Å)	
Ga–O1 = 1.881(11)	
Ga–O2 = 1.841(4)	
P–O1 = 1.486(9)	
P–O2 = 1.539(11)	
Typical bond angles (deg)	
Ga–O1–P = 132.37(75)	
Ga–O2–P = 131.98(56)	

$AlPO_4$. Besides, the irregular tetrahedra of the low cristobalite structure transform to regular ones in the high cristobalite structure. It can be mentioned here that the oxygen atoms in the high cristobalite structure occupy 1/3 of the available 48 (48h) positions [20]. However, the position of oxygen in the disordered site is restricted by considering the polyhedral nature, i.e., the positions which lead to the formation of an essentially regular polyhedra and less strained P–O–M linkages. This aspect of connectivities has been explained in the structural study of Ng and Calvo [20]. The typical Al–O bond lengths for $AlPO_4$ at 300°C is found to be 1.78 Å, whereas the Ga–O bond length for $GaPO_4$ at 700°C is 1.83 Å. At these two temperatures the high cristobalite lattice is observed for the corresponding phosphates.

The typical bond lengths of $AlPO_4$ and $GaPO_4$ at various temperatures are given in Table 5. A comparison of the XRD patterns shows that the stability of cubic phase of $GaPO_4$ increases with increase in Al^{3+} contents in the lattice. From the Figs. 3, 4 and 6 and

comparison of the α_V values (Table 3) of the cubic phases of various compositions it is observed that the average thermal expansion coefficients of the cubic phases increase with the addition of $GaPO_4$ to $AlPO_4$. This fact can be explained in terms of variation of the *M*–O–P bond angles in various compositions. A subtle increase or decrease in these bond angles may lead to correspondingly small positive or negative thermal expansion behavior. A comparison of the *M*–O–P bond angles of various compositions at a particular temperature suggests that there is a gradual increase in *M*–O–P bond angles with the increase in Al^{3+} content. The typical *M*–O–P bond angles of $AlPO_4$, $Al_{0.5}Ga_{0.5}PO_4$ and $GaPO_4$ at 700°C are 147.1°, 142.1° and 137.6°, respectively. It can be mentioned here that higher strained bond angle, in general expand due to the transverse vibration of the bridging oxygen atom. The relative increase of *M*–O–P bond angles with temperature will be more when this angle is smaller. Besides, the amplitude of thermal vibration of the bridging oxygen governs the extent of the dilation of *M*–O–P bond angle. Thus higher expansion is expected from the compounds with the lower values of bond angles, which may be a reason for higher thermal expansion coefficient of the cubic phase of Ga^{3+} containing compositions.

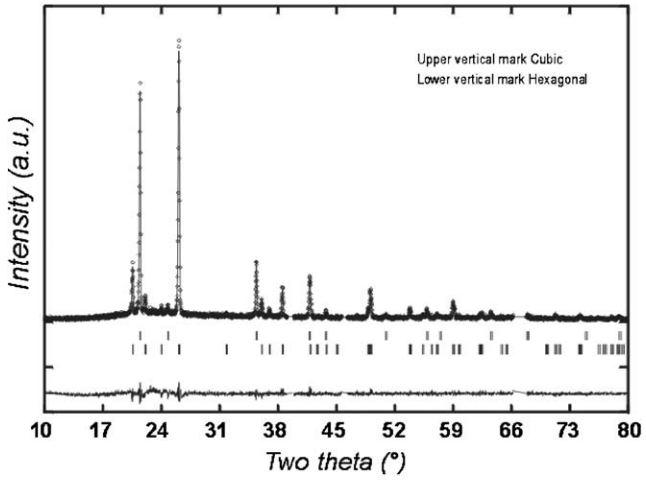

Fig. 8. A typical XRD pattern of $GaPO_4$ at 900°C.

It was observed that the variation of positional parameters at different temperatures does not reveal any definite correlation. But the overall thermal parameters of each composition are found to increase with temperature with a sharp increase at the phase transition. The typical variations of bond length of Al–O or Ga–O and P–O bonds for $AlPO_4$ and $GaPO_4$ are given in Table 5. From this table, it is apparent that there is no significant variation in the values of bond lengths. Thus based on the variation of bond lengths alone, one cannot explain the large difference in the thermal

Table 5
Typical *M*–O and P–O bond lengths (Å) and *M*–O–P bond angles (deg) of $AlPO_4$ and $GaPO_4$ with temperature

Temp. (°C)	$AlPO_4$			$GaPO_4$		
	Al–O	P–O	Al–O–P	Ga–O	P–O	Ga–O–P
25	1.75(1)	1.43(1)	147.1(6)	1.85(2)	1.52(2)	132.0(1.0)
	1.79(1)	1.52(1)	143.0(6)	1.85(2)	1.49(2)	132.5(9)
	1.77	1.475		1.85	1.505	
100	1.74(1)	1.42(1)	147.9(6)	1.83(2)	1.52(2)	134.6(1.0)
	1.80(1)	1.53(1)	143.9(6)	1.86(2)	1.47(2)	133.5(9)
	1.77	1.48		1.845	1.495	
200	1.75(1)	1.42(1)	150.4(9)	1.82(2)	1.52(2)	134.0(1.0)
	1.78(1)	1.51(2)	145.8(8)	1.86(2)	1.47(2)	134.9(9)
	1.77	1.47		1.84	1.495	
300	1.782(7)	1.457(6)	148.3(5)	1.84(2)	1.51(2)	134.4(1.0)
				1.86(2)	1.46(2)	135.2(1.0)
				1.85	1.485	
400	1.784(7)	1.459(6)	147.9(5)	1.83(2)	1.49(2)	136.4(1.0)
				1.84(2)	1.48(2)	137.1(1.0)
				1.85	1.485	
500	1.773(7)	1.471(6)	148.0(5)	1.80(2)	1.50(2)	137.4(1.1)
				1.84(2)	1.48(2)	137.7(1.1)
				1.82	1.49	
600	1.775(7)	1.470(6)	148.0(5)	1.84(2)	1.48(2)	138.8(1.2)
				1.81(2)	1.47(2)	140.4(1.2)
				1.825	1.475	
700	1.777(7)	1.476(6)	147.1(5)	1.83(3)	1.49(1)	137.6(2.0)
800	1.778(7)	1.474(6)	147.3(5)	1.84(2)	1.50(1)	136.5(1.7)
900	1.771(7)	1.471(6)	148.5(5)	1.83(3)	1.50(2)	137.0(2.3)
1000	1.778(7)	1.477(6)	146.9(5)	1.85(1))	1.47(1)	137.9(1.0)

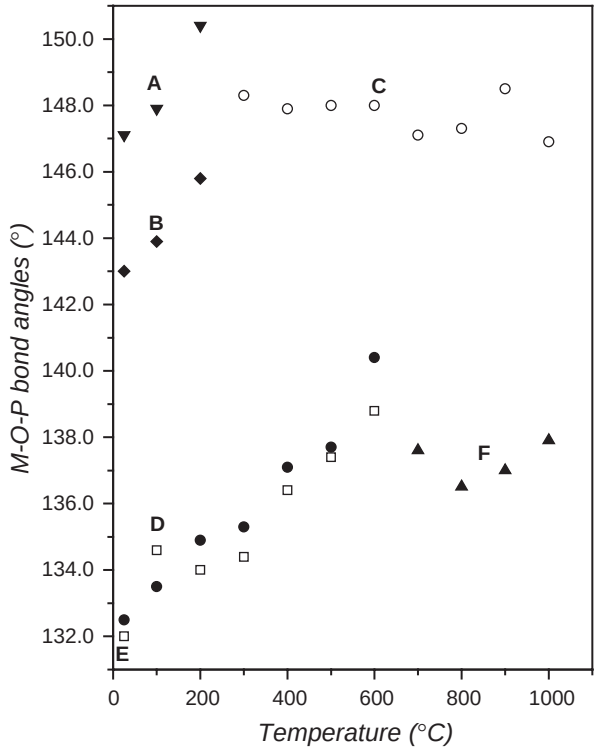

Fig. 9. Typical variation of M–O–P bond angles of $AlPO_4$ and $GaPO_4$ with temperature (std. deviations are shown in Table 5) A: Al–O1–P. B: Al–O2–P, C: Al–O–P, D: Ga–O1–P, E: Ga–O2–P, F: Ga–O–P.

expansion behavior of the orthorhombic and cubic phases. It may be noted that there is a systematic increase in the values of the M–O–P bond angles for the orthorhombic phase with increase in temperature up to the phase transition. In the cubic phase the M–O–P bond angles do not show any significant variation. The variation of the M–O–P bond angles with temperature (up to 1000°C) for $AlPO_4$ and $GaPO_4$ is shown in Fig. 9. The orthorhombic to cubic phase transition is observed within this temperature.

As explained in the last paragraph, an expansion in the bond angle leads to an increase in the separation of M and P cations, which in turn leads to a higher unit cell volume. The average inter-poyhedral angle has been quite often used to explain the thermal expansion behavior of framework lattices [1]. The M–O–P linkage will be free from any strain when it is close to 180°. Any deviation from this value will cause strain in it. To relax the strain of the M–O–P linkage, the linked polyhedra undergo correlated rotation so as to increase the bond angle. It has been reported that if the average bond angle is between 150° and 170°, then the bond angle decreases with increase in temperature and in turn the average $M-M'$ distance decreases. This is the most acceptable explanation of the NTE behavior of the ZrW_2O_8 and $Sc_3W_3O_{12}$ class of compounds [1,6]. However, the present observed M–O–P bond angles of the cubic phase of all the studied compositions are close to the lower limit of that in the NTE class materials. Hence in all the cases positive thermal expansions, though small, are observed. The feeble increase in the bond angle in the cubic phase of all the present compounds may be a possible explanation of the low thermal expansion of the cubic high temperature phase. In the orthorhombic phase of $AlPO_4$ it is observed that the average bond angle around O1 and O2 atoms are: 147.1° and 143.0° at 25°C and 150.4° and 145.8° at 200°C. The similar bond angles around O1 and O2 atoms in $GaPO_4$ are 132° and 132.5° at 25°C, which increase to 138.8° and 140.4° at 600°C. In the cubic phase the average bond angles around O atom are 148° for $AlPO_4$ and 137° for $GaPO_4$. The more strained bond angle in $GaPO_4$ explains the higher values of thermal expansion coefficients for $GaPO_4$ as compared to $AlPO_4$. A similar comparison of M–O–P angle with the composition can explain the smaller values of thermal expansion of the cubic phase of other compositions as well. It needs to be mentioned here that the thermal expansion coefficient values of the orthorhombic phase of $GaPO_4$ are lower than those of orthorhombic $AlPO_4$, even though the former has smaller inter-polyhedral angles. This may be because of the smaller amplitude of thermal vibrations of the $GaPO_4$ and other Ga^{3+} containing compositions as is seen from the overall thermal vibrations (Table 1) as well as the stability region of the orthorhombic phase.

The significant expansion of the unit cell volume causes a drastic decrease in the density of the unit cell, viz. X-ray densities of $AlPO_4$ at 25°C, 200°C and 300°C are 2.31, 2.27 and 2.17 gm/cm^3, respectively (orthorhombic at 25°C and 200°C and cubic at 300°C). X-ray densities of $GaPO_4$ at 25 (ortho.), 600 (ortho.) and 700°C (cubic) are 3.27, 3.16 and 2.98 gm/cm^3, respectively. In other words the β-phase (high cristobalite type) forms a low dense, i.e., loosely packed lattice, in which the different orientation (rocking motion) of the polyhedra are possible. This leads to lower expansion in the lattice. Since the increase in the M–O and P–O bond lengths are not significant in the studied temperature range, the thermal expansion of the lattice is mainly due to the orientation of the polyhedra, which is often compensated within a loosely packed lattice.

A comparison of the overall thermal expansion characteristics of the present studied cristobalite type phases to that of quartz type phase of the end members suggests that the thermal expansion of quartz type phases has smaller values. The typical coefficients of volume thermal expansion of $AlPO_4$ (Berlinite) and $GaPO_4$ (Quartz) are 81×10^{-6} (in 25–640°C) [18] and 42.8×10^{-6}/°C (in 25–900°C) [19], respectively. The phase transition behavior of the low quartz to high quartz structure of Berlinite ($AlPO_4$) and quartz type $GaPO_4$ have an almost similar behavior of thermal

expansion and phase transition as observed for low cristobalite phases in the present study.

The coefficient of thermal expansion and the range of stability of the cubic phase indicate that two opposite factors govern the transition temperature; namely, decrease in the average ionic radii of the metal ion and increase in the unit cell volume decrease the transition temperature. This suggests that substitution of the Al^{3+} with other smaller cation but increasing unit cell volume can retain the high cristobalite (cubic) phase or lower the transition temperature to room temperature. Attempts to stabilize the cubic phase by quenching the sample from higher temperature are not successful. The stabilization of the cubic phase at room temperature will have practical applications due to their smaller thermal expansion coefficients.

4. Conclusion

From the foregoing study the thermal expansion coefficients of the cristobalite type $AlPO_4$ and $GaPO_4$ as well as their solid solutions are determined. In all the cases the low cristobalite (orthorhombic) lattice transforms to the high cristobalite (cubic) lattice. The transformation of the low cristobalite to the high cristobalite lattice is accompanied by a drastic expansion of the unit cell volume, there by causing a significant decrease of the density of the lattice. The low dense loosely packed lattice of the high cristobalite has significantly lower thermal expansion coefficients in contrast to the low the low cristobalite lattice. The increase of the ionic radii form Al^{3+} to Ga^{3+} is reflected in the increase of this transition temperature. Within the orthorhombic phase the coefficients of thermal expansion decrease with the increase in Ga^{3+} content in the lattice, whereas reverse phenomena is observed with in the cubic phase.

Acknowledgments

The authors thank Dr. N.M. Gupta, Head Applied Chemistry Division for his keen interest in this work. Also Mr. B.R. Ambekar is thanked for his help in recording the high temperature XRD patterns.

References

[1] J.S.O. Evans, T.A. Mary, A.W. Sleight, J. Solid State Chem. 133 (1997) 580.
[2] P.M. Forster, A. Yokochi, A.W. Sleight, J. Solid State Chem. 140 (1998) 157.
[3] D.A. Woodcock, P. Lightfoot, C. Ritter, Chem. Commun. 107 (1998).
[4] V. Korthius, N. Khorsrovani, A.W. Sleight, N. Robert, R. Dupree, W.W. Warren, Chem. Mater. 7 (1995) 412.
[5] P. Lightfoot, D.A. Woodcock, J.D. Jorgensen, S. Short, Int. J. Inorg. Mater. 1 (1999) 53.
[6] J.S.O. Evans, T.A. Mary, T. Vogt, M.A. Subramanian, A.W. Sleight, Chem. Mater. 8 (1996) 2809.
[7] D. Taylor, J. Br. Ceram. Trans. 83 (1984) 129.
[8] K. Rottger, A. Endriss, J. Ihringer, S. Doyle, W.F. Khuss, Acta Cryst. B50 (1994) 644.
[9] P. Tachaufeser, S.C. Parker, J. Phys. Chem. 99 (1995) 10600.
[10] M.P. Attfield, A.W. Sleight, Chem. Commun. 601 (1998).
[11] F.A. Hummel, J. Am. Ceram. Soc. 32 (1949) 320.
[12] A. Perloff, J. Am. Ceram. Soc. 39 (1956) 83.
[13] W.R. Beck, J. Am. Ceram. Soc. 32 (1949) 147.
[14] E. Schaffer, R. Roy, J. Am. Ceram. Soc. 39 (1956) 330.
[15] M.J. Burger, Am. Minerol. 33 (1948) 751.
[16] R.C.L. Mooney, Acta Cryst. 9 (1956) 728.
[17] R.D. Shanon, Acta Cryst. A32 (1976) 751.
[18] M.K. Kihara, Can. Miner. 24 (1997) 243.
[19] P. Worsch, B. Koppenlhuber-Bitschnau, F.A. Mautner, P.W. Krempl, W. Wallnofer, Mater. Sci. Forum 278–281 (1998) 600.
[20] H.N. Ng, C. Calvo, Can. J. Phys. 55 (1977) 677.
[21] P. Worsch, B. Koppenlhuber-Bitschnau, F.A. Mautner, P.W. Krempl, W. Wallnofer, P. Doppler, J. Gautsch, Mater. Sci. Forum 312–324 (2000) 914.
[22] J. Rodriguez-Caravajal, Sattelite Meeting on Powder Diffraction, 15th Conference of the International Union of Crystal, Vol. 127, Toulouse France, 1990, p. 23.
[23] S.K. Kulshreshtha, O.D. Jayakumar, V. Sudarshan, J. Phys. Chem. of Solids, submitted.
[24] A.F. Wright, A.J. Leadbetter, Philos. Mag. 31 (1975) 1391.
[25] A. Goiffon, J.-C. Jumas, M. Maurin, E. Philippot, J. Solid State Chem. 61 (1986) 384.
[26] K. Kosten, H. Arnold, Z. Kristallogr. 152 (1980) 119.
[27] L.H. Cohen, W. Klement, Philos. Mag. A39 (1979) 399.
[28] D. Cachau-Hervellat, J. Bennazha, A. Goiffon, A. Ibanenz, E. Phillipot, Eur. J. Solid State Chem. 29 (1992) 1295.
[29] D.M. Hatch, S. Ghose, J.L. Bjorkstam, Phys. Chem. Minerals 21 (1994) 67.